SEMARAK ILMU PUBLISHING

Semarak Engineering Journal

Journal homepage:
https://semarakilmu.my/index.php/sej/index
ISSN: 3036-0145

Parametric Study of Hybrid Composites for Automotive Bumper Application

Muhammad Na'iim Mohd Rafi[1], Yulfian Aminanda[2,*]

[1] Brunei Shell Petroleum Co. Sdn. Bhd., Jalan Utara, Panaga, Seria, Brunei Darussalam
[2] Mechanical Engineering Department, Universiti Teknologi Brunei, Brunei Darussalam

ARTICLE INFO

Article history:
Received 15 August 2025
Received in revise 16 September 2025
Accepted 25 September 2025
Available online 22 December 2025

Keywords:
Finite element analysis; front bumper; hybrid composite; natural fiber; impact engineering; energy absorption

ABSTRACT

With the surge in vehicle ownership coupled with rising concern towards environmental impacts, there is a pressing need to develop a fuel-efficient vehicle with assurance of crashworthiness and pedestrian safety. Front bumper beam, an energy absorbing component of the front bumper system, exhibit ample potential for the implementation of sustainable and lightweight materials. This study explored the feasibility of 16 plies of hybrid natural/synthetic composite for bumper beam application through finite element analysis. The simulation was performed using Ansys LS-DYNA with the test conditions in accordance with the Euro NCAP full-width frontal impact test. Based on the parametric studies conducted with different fibre orientations, stacking configuration, fibre materials and ply thickness, hybrid glass/flax composite bumper beam was deemed as the best hybrid composite with a configuration of ($G[\pm45°]_4$ $F[\pm45°]_4$ $F[0°/90°]_4$ $G[0°/90°]_4$). The crashworthiness of the composite proved to be superior to the conventional DP1400 bumper beam, displaying comparable specific energy absorption of around 12.65 kJ/kg while substantially reducing the peak force by from 2380 to 993 kN at the expense of reduced energy absorption capability and increased in thickness. All in all, this study accentuates the viability of hybrid glass/flax composite to substitute conventional steel in bumper beam applications.

1. Introduction

Front bumper beam is the primary component in a front bumper system that absorbs the impact energy and provides bending resistance before distributing the residual energy to other parts of the car [1]. Conventional bumper beam is primarily composed of metallic materials such as high-strength steel. However, concerns relating to environmental impacts intensified the need of developing vehicles with exceptional fuel economy while maintaining exceptional crashworthiness.

Synthetic composite subjected to impact loading has been studied extensively, i.e by Safri S.N.A *et al*. [2]. The same case for natural fibre composite under the same loading [3] and even using honeycomb structure of sandwich structure [4].

* *Corresponding author.*
E-mail address: yulfian.aminanda@utb.edu.bn

https://doi.org/10.37934/sej.10.1.7687

Hybrid natural/synthetic composite offer a promising solution to achieve a compromise between crashworthiness, fuel economy, and sustainability as evaluated by Chandgude *et al.* [5]. Despite this, limited literatures are available on direct assessment of hybrid natural/synthetic composite for bumper beam applications. Furthermore, performance comparison between natural fibers to be hybridized with synthetic fibers through bumper beam simulations remain obscure.

The principal focus of this study is to investigate the feasibility of hybrid natural/synthetic composite as a sustainable and lightweight alternative to steel for bumper beam application through finite element analysis. Additionally, parametric studies for the hybrid composite are completed to ensure that the eventual hybrid composite can produce comparable results to steel bumper beam. This also includes the provision of direct comparison between the performance of different natural fibers.

2. Methodology

The simulations performed in this study utilized LS-PrePost as the primary software for pre-processing and post-processing of the bumper beam models while numerical solutions were computed through Ansys LS-DYNA. Ansys LS-DYNA was selected as the processing software since Ansys LS-DYNA specializes in solving dynamic simulations using explicit time integration which is essential since crash events occur in milliseconds with high strain rates, the explicit time integration allows for relatively accurate prediction of crash behaviour [6].

2.1 Bumper Beam And Material Modelling

The bumper beam model was adapted from the works of Abrar *et al.* [7] and Godara and Nagar [8] with the relevant dimensions shown in Figure 1. In LS-PrePost, the bumper beam model was meshed uniformly using 4-node Belytschko-Tsay shell element since the thickness of bumper beam is relatively lower than other dimensions of the model. Similarly, the crash box was also modelled using this element with a fixed mesh size of 10 mm. Note that the mesh size for the bumper beam was evaluated through a mesh convergence study.

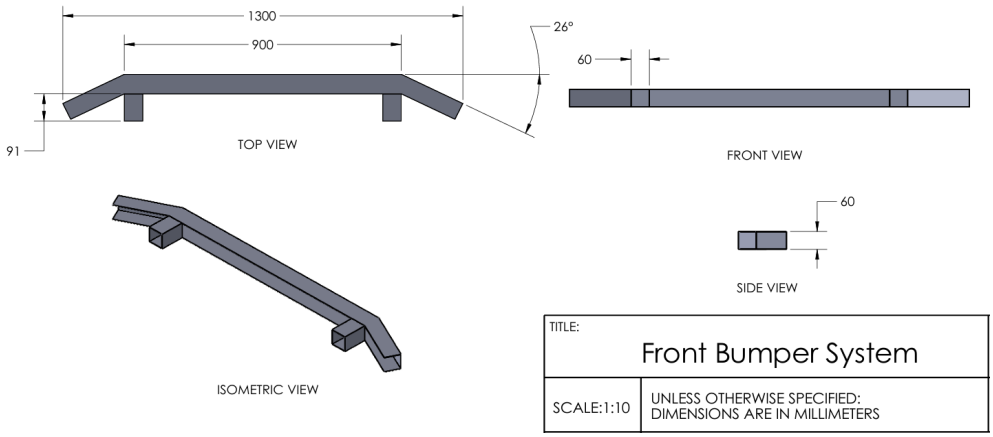

Fig. 1. Dimensions of bumper beam model.

DP1400 high-strength steel with a thickness of 2.00 mm was selected as the baseline material for the bumper beam, represented as MAT024 (Linear Piecewise Plasticity) in the simulation. For the hybrid natural/synthetic composite, only glass fiber was considered as the synthetic fiber with hemp, flax, and kenaf as the potential natural fibers to be hybridized with the glass fibers. To limit the scope

of the study, the matrices for all fibers were limited to epoxy while ply thicknesses for all fibers were assigned to a fixed value of 0.285 mm unless specified. The composite was applied to the bumper beam using *PART_COMPOSITE function and was modelled using MAT054 (Enhanced Composite Damage) with Chang-Chang matrix failure mode. Essential composite material properties used in the simulations are summarized in Table 1.

Table 1
Properties of woven synthetic composite (glass/GFRE) and woven natural composite (hemp/HFRE, flax/FFRE and kenaf/KFRE) used in the simulations

Properties	GFRE [9]	HFRE [9]	FFRE [10]	KFRE [11]
Density, ρ (kg/m^3)	1942	1298	1270	1180
Longitudinal Young's Modulus, E_1 (GPa)	18.04	5.88	9.9	6.0
Longitudinal Tensile Strength, X_t (Mpa)	415	62.48	138	35
Longitudinal Compressive Strength, X_c (Mpa)	200	54.99	99	76
Transverse Young's Modulus, E_2 (GPa)	18.04	5.65	9.0	6.0
Transverse Tensile Stength, Y_t (Mpa)	415	62.48	138	35
Transverse Compressive Strength, Y_c (Mpa)	200	54.99	99	76
Shear Modulus, G_{12} (GPa)	2.22	1.2	1.7	1.4
Shear Strength, S_c (Mpa)	75	46.75	40	30
Poisson's Ratio, v_{12}	0.100	0.085	0.120	0.221

2.2 Verification and Validation of Models

The results from the bumper beam modelled were verified through mesh convergence study to select the best size of shell elements for the bumper beam. This was completed to balance the computational efficiency with results accuracy. Additionally, due to the complex behaviour of composite, validation for the composite material model was performed based on the drop-weight impact test performed by Nawawithan *et al.* [9] according to ASTM-D7136 standard. This ensures that the composite material modelled through MAT054 can predict the behaviour of actual composites accurately with acceptable deviations.

In the experiment, 16 plies of woven GFRE with an arrangement of $[\pm45°, 0°/90°]_8$ were tested for energy levels of 34J and 50J. The impactor was modelled using MAT020 while MAT054 was used to model the composite with automatic surface to surface contact for the contact between the impactor and the laminate. The modelling of the 16 plies of composite was completed through the *PART_COMPOSITE function. Both energy level used an impactor with a mass of 9.17 kg, corresponding to an initial velocity of 2.72 m/s and 3.30 m/s respectively. The individual thickness of the ply was 0.285 mm, resulting in the total thickness to be 4.56 mm. Figure 2 illustrates the simulation setup for the drop-weight impact test.

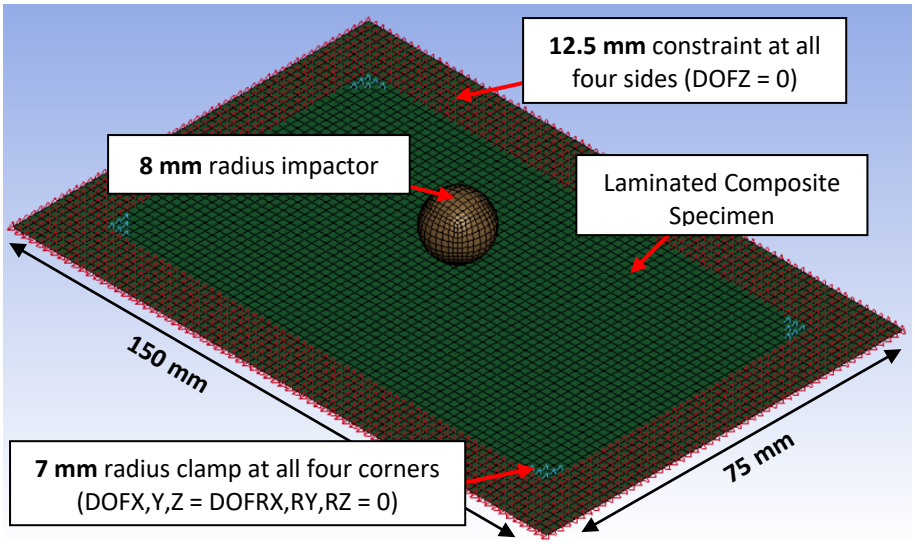

Fig. 2. Simulation setup showing the relevant dimensions and boundary conditions applied for composite model validation.

2.3 High-Velocity Impact Test Modelling

In this study, the simulations were performed according to Euro NCAP full-width frontal impact test standard [12]. For this test, the bumper system was set to move towards a 1500 mm x 750 mm x 5 mm rigid wall at 50 km/h as illustrated in Figure 3. The solid, rigid wall was represented using MAT020 (Rigid) while a mass element was attached to the crash box through *CONSTRAINED_NODAL_RIGID_BODY function. This mass represents the mass of the vehicle which was assumed to be 1400 kg (mass of TATA Indica). The integration of this function provided a physical connection from the lumped rigid node to the bumper system, causing the mass and bumper system to move simultaneously while allowing the mass to influence the deformation in the bumper system.

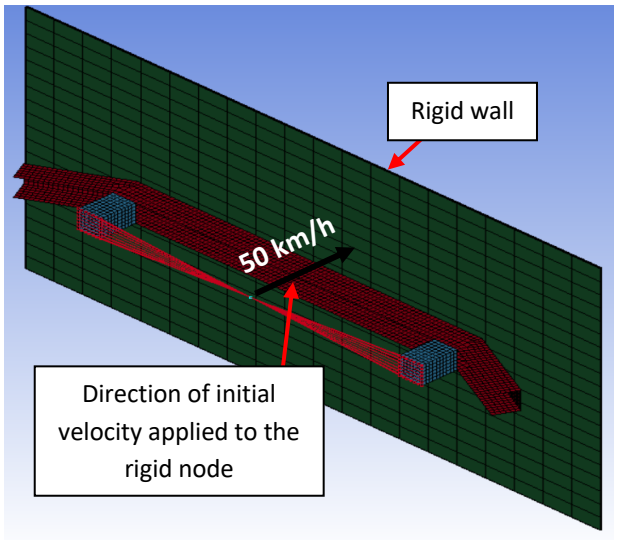

Fig. 3. Simulation setup based on Euro NCAP full-width frontal impact test.

*AUTOMATIC_SURFACE_TO_SURFACE contact was used for the collision between the bumper beam with wall, crash box with wall, and crash box with bumper beam. To prevent unrealistic contacts within parts caused by the severity of collision at high velocity, *AUTOMATIC_SINGLE_SURFACE was included for bumper beam and crash box. Lastly, through

intensive iterations, the common surface between the crash box and bumper beam was ideally bonded using *AUTOMATIC_TIED_SHELL_EDGE_TO_SURFACE contact.

2.4 Parametric Study For Composite

The generation of the best hybrid natural/synthetic composite were performed sequentially. First, best fiber orientations were evaluated using 16 plies of pure woven glass fibers, followed by determination of the ideal stacking sequence using 8 plies of hemp fibers and 8 plies of glass fibers. Afterwards, the hemp fibers were substituted with flax and kenaf. Hemp, flax, and kenaf were selected as the optimal natural fibers to be hybridized with the glass fiber following the findings from Balakrishnan *et al.* [13] to achieve a compromise between mechanical properties, density, and availability of the fibers in Malaysia. Finally, the best thickness for the hybrid natural/synthetic composite bumper beam was assessed by adjusting the ply thickness.

Parameters varied in this study are shown in Table 2. Key assessment factors for all parameters investigated include energy absorption (E_a), specific energy absorption (*SEA*), and maximum impact force (F_{max}).

Table 2
Configurations of composite for the parametric study

Fiber Orientations		Stacking Sequences		Natural Fibers		Ply Thickness	
F1	$[0°/90°]_{16}$	S1	G/H/H/G	H1	Hemp	T1	0.185
F2	$[\pm45°]_{16}$	S2	H/G/G/H	H2	Flax	T2	0.285
F3	$[(0°/90°)_4\,(\pm45°)_4]_s$	S3	G/H/G/H	H3	Kenaf	T3	0.385
F4	$[(\pm45°)_4\,(\pm45°)_4]_s$	S4	H/G/H/G			T4	0.485
F5	$[0°/90°]_8\,[\pm45°]_8$					T5	0.585
F6	$[\pm45°]_8\,[0°/90°]_8$					T6	0.685
F7	$[\pm45°]_4\,[0°/90°]_4\,[\pm45°]_4\,[0°/90°]_4$						
F8	$[0°/90°]_4\,[\pm45°]_4\,[0°/90°]_4\,[\pm45°]_4$						

3. Results and Discussion

3.1 Verification and Validation Results

For mesh convergence, based on the internal energy-time graph presented in Figure 4, internal energy for element sizes of 10, 8, and 6 mm reached a plateau of around 47 kJ with minimal discrepancies in the range of 2.3% to 2.9%. These remaining deviations can be attributed to the complexity of the response of the bumper beam during high-velocity crash events, causing minor deviations to occur in the behaviour of the bumper beam elements. Additionally, all mesh sizes exhibited similar trend in internal energy. Hence, 8 mm was chosen as the optimal mesh size for the bumper beam to compromise between accuracy of results and computational cost.

As for the validation, the results demonstrated in Figure 5 showed that the simulated composite model produced similar behaviour in internal energy, absorbing 11.1 J and 20.3 J of energy for impact

energy levels of 34 J and 50 J respectively. As the calculated percentage error was lower than 15% for both levels (8.9% for 34 J and 11.7% for 50 J), the MAT054 modelled was deemed acceptable. Errors present in the results were attributed to the following simplifications:

1. The element deletion parameters in MAT54 (DFAILT, DFAILC, DFAILS, DFAILM and EFS) were not explicitly defined in the validation paper. Thus, all stated parameters were assumed to be in unity throughout the simulations. Note that the element deletion parameters must be determined through experimentation.
2. Damage progression parameters for the GFRE composite in tension and compression (SLIMT1, SLIMT2, SLIMC1 and SLIMC2) were assumed to be equal with an adjusted value of 0.7. Additionally, damage progression parameter in shear (SLIMS) was assumed to be unity. Note that damage progression parameters can be evaluated through curve-fitting experimental and simulation results.
3. The simulations did not take into account delamination between each layer since *PART_COMPOSITE and single shell layer approach was used to define the composite laminates. Therefore, this approach assumes that each layer is perfectly bonded to each other.

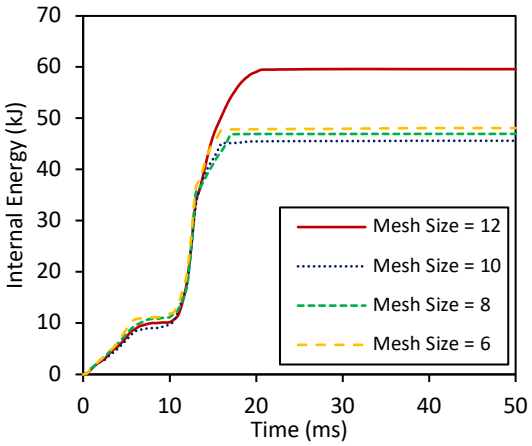

Fig. 4. Internal energy-time graph for mesh convergence study.

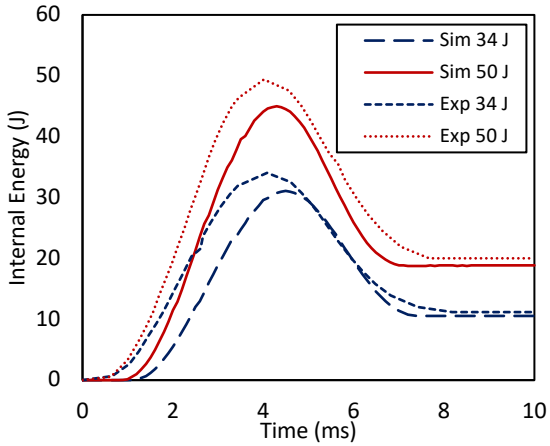

Fig. 5. Internal energy-time graph for composite material model validation.

3.2 Fiber Orientations Analysis

Shown in Figure 6 is the results obtained according to different combinations of fiber orientations. Based on the results in Figure 6 (a), the presence of ±45° as the outermost layers generally improved the energy absorption capacity. This was attributed to the balanced capability of the ±45° fibers to handle multi-directional stress upon impact with the rigid wall. By placing the ±45° fibers on the outer layers, most of the impact energy was reduced before reaching the inner layers, allowing the inner layers to absorb more energy. Similar observation was noted based on a drop-weight impact test in [9] whereby in-plane shearing effect of ±45° fibers enhanced energy absorption through fiber and matrix deformation.

However, as shown in Figure 6 (b), several configurations with ±45° fibers as the outermost layer (F2, F4 and F7) suffered impact forces ranging from 3.5% to 5.8% (higher than 1364 kN). Only three fiber arrangements experienced a maximum impact force of lower than 1400 kN which are F3, F5, and F6. This implies that although the ±45° fibers can distribute energy more effectively, the fiber

orientations should only be arranged in a ±45° orientations successively up to 8 plies to prevent excessive transfer of impact force.

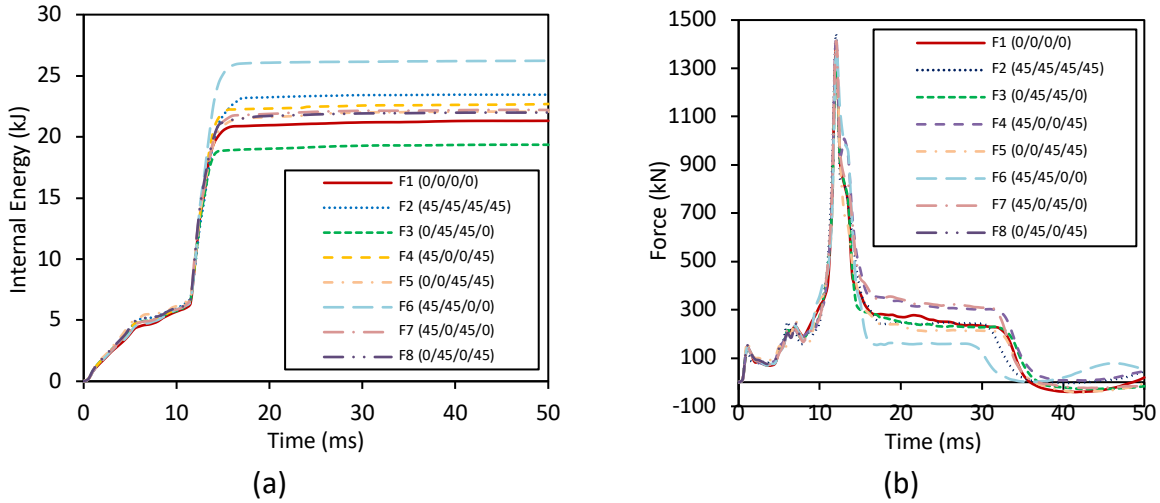

Fig. 6. Graphs for fiber orientations where (a) Internal energy-time graph, and (b) Force-time graph

Further examinations on the maximum Von Mises stresses experienced in each layer as illustrated in Figure 7 revealed that the outermost and innermost layers were subjected to higher stresses as opposed to the middle layers. Therefore, the synthetic fibers should be placed as the outer and inner layers with the natural fibers in the middle fibers to maximize energy absorption capabilities and minimize failure particularly for low-velocity collisions. Nonetheless, it can be deduced that arrangement F6, $[\pm 45°]_8$ $[0°/90°]_8$, outperformed other combinations, absorbing the highest amount of impact energy (26.23 kJ) while transferring comparatively low impact force (1364 kN).

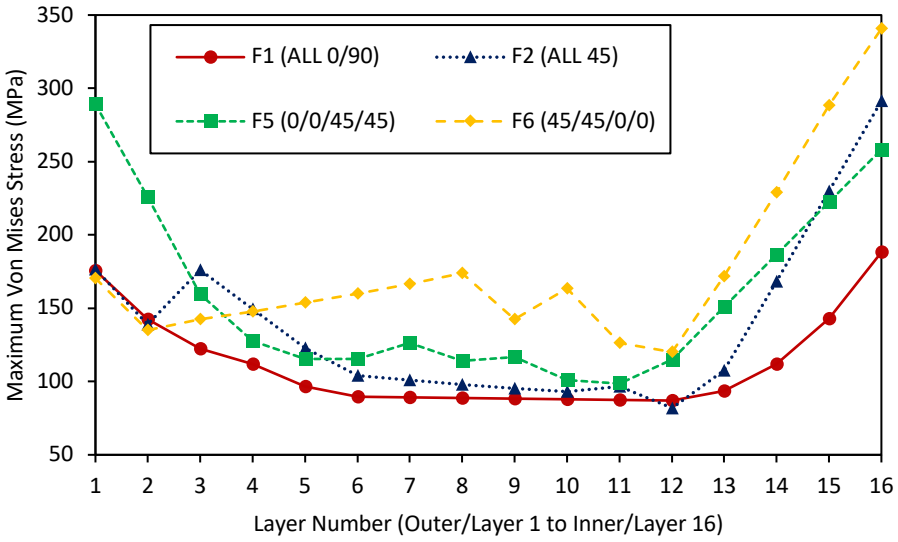

Fig. 7. Graph for maximum Von Mises stress experienced according to each layer based on selected fiber orientations

3.3 Stacking Sequence Analysis

The internal energy and force results for varying stacking sequences of hybrid glass/hemp composite are presented in Figure 8. Generally, stacking configurations with hemp fibers as the outermost layer (S2 and S3) performed poorly based on the amount of energy absorbed, around 8.3% to 10.7% lower than S1 and S4. The difference in energy absorbed can be attributed to the reduction in flexural properties of the hybrid composite due to the placement of the weaker fibers on the outer layers. This finding is supported by the experimental study conducted by Ramesh *et al.* [14] which showed that sequences with weaker, woven ramie fibers on the outermost layer absorbed lower energy relative to arrangements with basalt fibers as the outer layer.

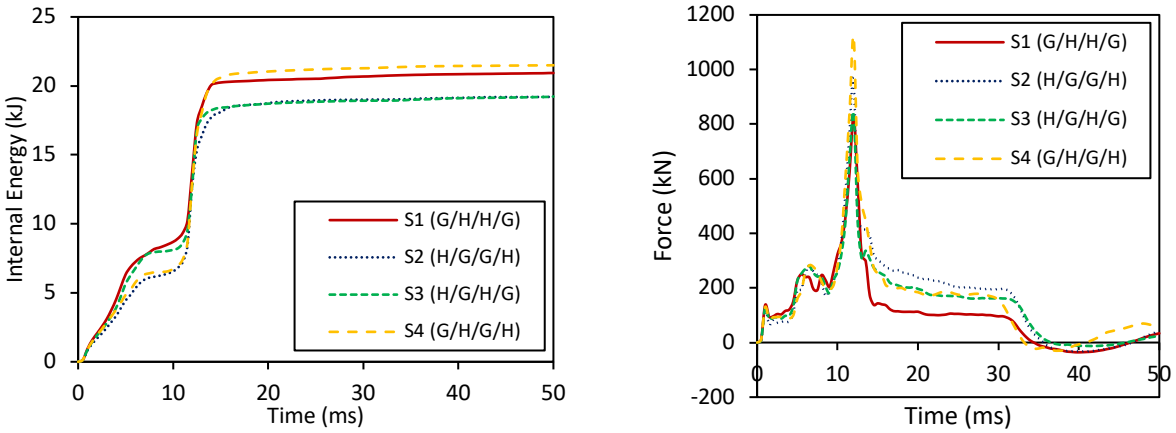

Fig. 8. Graphs for stacking sequences where (a) Internal energy-time graph, and (b) Force-time graph

Despite S4 exhibiting superior energy absorption capability, S4 also experienced the highest impact force with a value of 1119 kN, around 17% to 35% greater than maximum force in other stacking sequences. This excessive force can impose severe injuries onto the vehicle occupants. Furthermore, according to the stresses trend defined in Figure 7, placing the weaker hemp fibers as the innermost layer may lead to premature failure. Therefore, the sandwich stacking sequence S1, $G[\pm45°]_4$ $H[\pm45°]_4$ $H[0°/90°]_4$ $G[0°/90°]_4$, was deemed as the best stacking sequence for the hybrid composite, experiencing the least impact force (829 kN) while absorbing 20.93 kJ of energy.

3.4 Natural Fiber Analysis

As the ply thickness for all fibers were controlled at 0.285 mm, the disparity in results for natural fibers is only dependent on the mechanical properties of each fiber. Overall, in terms of energy absorbed through deformation illustrated in Figure 9 (a), H2 outperformed other hybrid composites with a cumulative energy absorbed of 22.39 kJ. This resulted in an energy absorption to mass ratio of 12.65 kJ/kg, 2.0% to 8.2% higher than H3 and H1 respectively. The stated outcome was anticipated as this reflects the superior mechanical properties (strengths and moduli) of flax in contrast to hemp and kenaf.

However, as shown in Figure 9 (b), Flax transferred the highest impact force at around 993 kN. This suggests that although most of the energy can be dissipated through FFRE bumper beam, this benefit comes at the expense of higher impact force, increasing the risk of inflicting injuries to vehicle

occupants. Nonetheless, as the impact force experienced by H2 is 27.2% lower than the maximum crash force transmitted by pure GFRE (1364 kN), H2 is chosen as the best hybrid natural/synthetic composite. It must be noted that flax can be substituted with kenaf if further reduction in maximum impact force by more than 20.7% (from 993 to 787 kN) is required.

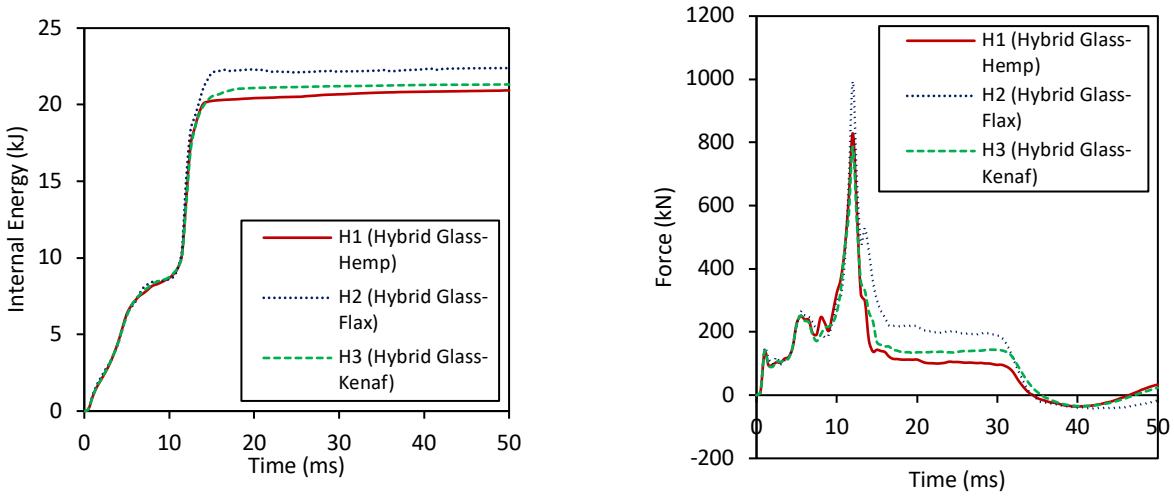

(a) (b)

Fig. 9. Graphs for natural fibers where (a) Internal energy-time graph, and (b) Force-time graph

3.5 Thickness Analysis

Figure 10 provides the combination of overall results as a function of bumper beam thickness which differ according to different ply thickness. Comparing the energy absorption capacity of varying ply thicknesses shown in the figure, the rise in bumper beam thickness improved the energy absorption capability. However, the maximum impact force experienced by the bumper beam experienced a steady rise as the bumper beam thickness increased, similar to the observations made by Zhu *et al.* [15].

Since higher impact forces are detrimental to the safety of occupants, thicknesses from T3 to T6 which experienced greater impact force values than the best pure glass fibers (1364 kN) were excluded from the potential thickness of the bumper beam. Referring to the specific energy absorption capabilities of varying bumper beam thicknesses provided, a stable decreasing trend was observed, indicating that increasing the thickness generally reduces the efficiency in amount of energy absorbed per unit mass. Based on the trend in E_a and *SEA* illustrated in Figure 10, a compromise between energy absorption and energy absorption per unit mass can be achieved at the intersection of E_a and *SEA* series. Nonetheless, as this value was not evaluated, T1 and T2 emerge as the potential best thickness for the hybrid composite bumper beam to maximize the amount of energy absorbed per unit mass.

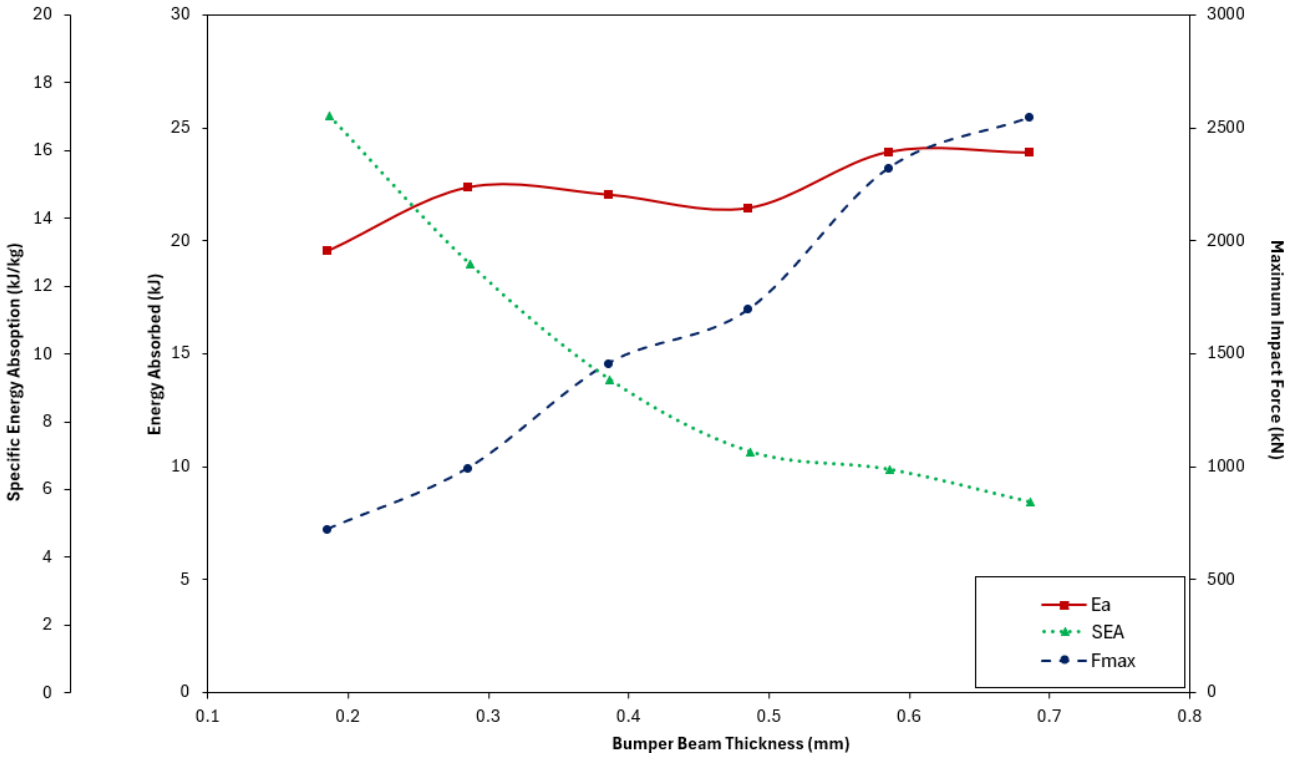

Fig. 10. E_a, *SEA*, and F_{max} values obtained from varying bumper beam thickness

Through direct comparison of the performance for T1 and T2, it was observed that increasing the thickness from T1 to T2 resulted in 14.4% rise in E_a (from 19.57 to 22.39 kJ) and 25.7% reduction in *SEA* (from 17.02 to 12.65 kJ/kg) while causing a surge of 37.3% in F_{max} (from 723 to 993 kN). Despite the lower specific energy absorption and higher impact force transmitted in T2, as deflection must be considered for low-velocity crash scenario, T2 is deemed as the best thickness for the hybrid composite bumper beam.

3.6 Performance Comparison With Steel

Shown in Figure 11 is the comparison between internal energy and force behaviour of the best hybrid composite (G[±45°]$_4$ F[±45°]$_4$ F[0°/90°]$_4$ G[0°/90°]$_4$) to DP1400 bumper beam. Although similar behaviour was observed for both materials, the results presented showed that in a high-velocity collision, usage of hybrid composite led to a 58.3% (from 2380 to 993 kN) reduction in impact force transmitted (Figure 11 (b)) and a 2.3% (from 12.36 to 12.65 kJ/kg) improvement in specific energy absorption. Despite the enhancement in specific energy absorption, steel remained superior in the energy absorption capability aspect, absorbing 52.3% (46.96 kJ for DP1400 and 22.39 kJ for hybrid glass/flax composite) more energy than the hybrid composite bumper beam as shown in Figure 11 (a).

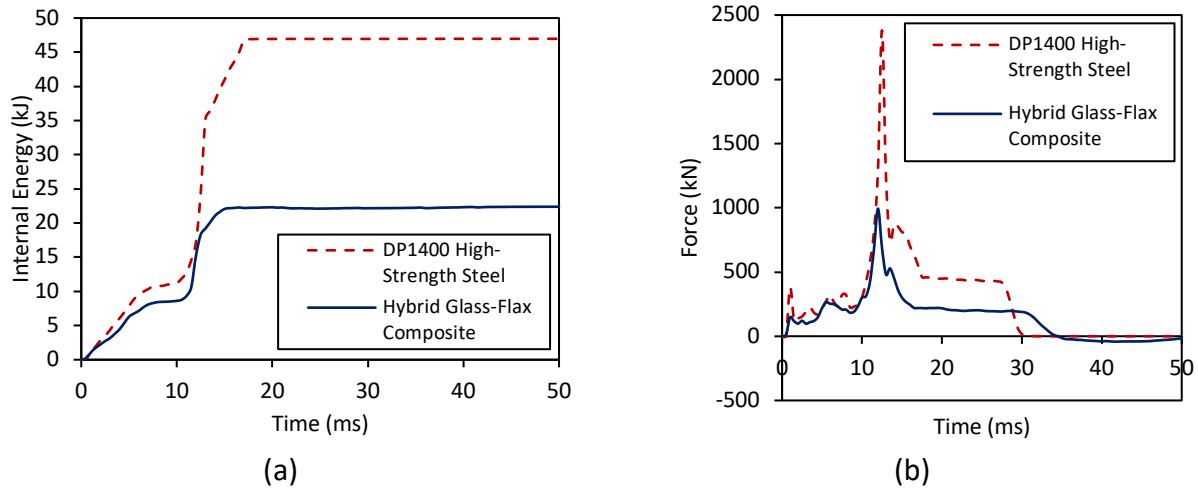

Fig. 11. Graphs for performance comparison between hybrid natural/synthetic composite and DP1400 where (a) Internal energy-time graph, and (b) Force-time graph

Overall, it can be concluded the hybrid glass/flax composite bumper beam enhanced the crashworthiness by reducing the impact force transmitted through the bumper beam. Furthermore, the integration of hybrid composite onto the bumper beam resulted in 53.4% (From 3.80 to 1.77 kg) reduction in mass while sustaining sufficient energy absorption capability of more than 20.25 kJ (15% of the initial kinetic energy of the vehicle which was around 135 kJ), improving the *SEA*. This accentuates the future of composite for bumper beam applications as a lightweight yet strong alternative, improving both crashworthiness and fuel economy of a vehicle.

Nonetheless, care must be taken when designing hybrid glass/flax bumper beam as the thickness of the composite bumper beam is 4.56 mm, roughly 2.3 times more than DP1400 steel bumper beam. This rise in thickness may limit the space availability for other components of the car.

4. Conclusion

Based on the cumulative configurations analysis, $G[\pm45°]_4$ $F[\pm45°]_4$ $F[0°/90°]_4$ $G[0°/90°]_4$ with a ply thickness of 0.285 mm was concluded as the best hybrid natural/synthetic composite for bumper beam application. Performance of the hybrid composite provided comparable specific energy absorption capability to the high-strength steel while reducing peak force transferred. Overall, integration of the hybrid glass/flax synthetic proved to be beneficial for crashworthiness and reduction in weight purposes, highlighting hybrid natural/synthetic composite as a viable alternative to replace steel for bumper beam application.

Acknowledgement

This research was not funded by any grant.

References

[1] M. S. Nasiruddin, H. A., R. J., W. W. S., and A. M. N., "A Review of Energy Absorption of Automotive Bumper Beam," Jan. 2017. [Online]. Available: (PDF) A Review of Energy Absorption of Automotive Bumper Beam (accessed Sep. 26, 2024)

[2] Safri S.N.A, Sultan M.T.H, Aminanda Y., "Impact characterisation of Glass Fibre Reinforced Polymer (GFRP) type C-600 and E-800 using a drop weight machine", 2014. Applied Mechanics and MaterialsConference PaperOpen Access2014, DOI: https://doi.org/10.4028/www.scientific.net/AMM.629.461

[3] Ghazilan, A.L. A, Mokhtar H., Shaik Dawood M.S.I., Aminanda Y., "Tensile Mechanical Property of Oil Palm Empty Fruit Bunch Fiber Reinforced Epoxy Composites", 2017, IOP Conference Series: Materials Science and EngineeringConference PaperOpen Access2017, DOI: http://dx.doi.org/10.1088/1757-899X/184/1/012046

[4] Kadir Nurdina Abd, Aminanda Yulfian, Dawood Mohd Sultan Ibrahim Shaik, Mohktar Hanan, "Numerical Analysis of Kraft Paper Honeycomb subjected to uniform compression loading", Journal of Physics: Conference SeriesConference PaperOpen Access2017, DOI: https://dx.doi.org/10.1088/1742-6596/914/1/012004

[5] S. Chandgude and S. Salunkhe, "In state of art: Mechanical behavior of natural fiber-based hybrid polymeric composites for application of automobile components," Polym Compos, vol. 42, no. 6, pp. 2678–2703, Jun. 2021, doi: https://doi.org/10.1002/pc.26045

[6] D. Jan, M. S. Khan, I. Ud Din, K. A. Khan, S. A. Shah, and A. Jan, "A review of design, materials, and manufacturing techniques in bumper beam system," Composites Part C: Open Access, vol. 14, p. 100496, Jul. 2024, doi: https://doi.org/10.1016/j.jcomc.2024.100496

[7] M. S. Ul Abrar, K. F. Nadim Ezaz, M. J. Hasan, R. I. Pranto, T. A. Alvy, and M. Z. Hossain, "Speed-dependent impact analysis on a car bumper structure using various materials," Results in Engineering, vol. 21, Mar. 2024, doi: https://doi.org/10.1016/j.rineng.2024.101927

[8] S. S. Godara and S. N. Nagar, "Analysis of frontal bumper beam of automobile vehicle by using carbon fiber composite material," in Materials Today: Proceedings, Elsevier Ltd, 2019, pp. 2601–2607. doi: https://doi.org/10.1016/j.matpr.2020.02.550

[9] N. Nawawithan, P. Kittisakpairach, S. Nithiboonyapun, K. Ruangjirakit, and P. Jongpradist, "Design and performance simulation of hybrid hemp/glass fiber composites for automotive front bumper beams," Compos Struct, vol. 335, May 2024, doi: https://doi.org/10.1016/j.compstruct.2024.118003

[10] G. Del Bianco et al., "Low-Velocity Impact of carbon, flax, and hybrid composites: Performance comparison and numerical modeling," Compos Struct, vol. 344, p. 118318, Sep. 2024, doi: https://doi.org/10.1016/j.compstruct.2024.118318

[11] M. J. Sharba, Z. Leman, M. T. H. Sultan, M. R. Ishak, and M. A. A. Hanim, "Tensile and Compressive Properties of Woven Kenaf/Glass Sandwich Hybrid Composites," Int J Polym Sci, vol. 2016, pp. 1–6, Mar. 2016, doi: http://dx.doi.org/10.1155/2016/1235048

[12] Euro NCAP, "European New Car Assessment Programme (Euro NCAP) Full Width Frontal Impact Testing Protocol," Nov. 2015. [Online]. Available: full-width-frontal-impact-test-protocol-v102.pdf (accessed Sep. 20, 2024)

[13] T. S. Balakrishnan et al., "Selection of Natural Fibre for Pultruded Hybrid Synthetic/Natural Fibre Reinforced Polymer Composites Using Analytical Hierarchy Process for Structural Applications," Polymers (Basel), vol. 14, no. 15, p. 3178, Aug. 2022, doi: https://doi.org/10.3390/polym14153178

[14] V. Ramesh, K. Karthik, R. Cep, and M. Elangovan, "Influence of Stacking Sequence on Mechanical Properties of Basalt/Ramie Biodegradable Hybrid Polymer Composites," Polymers (Basel), vol. 15, no. 4, p. 985, Feb. 2023, doi: https://doi.org/10.3390/polym15040985

[15] G. Zhu, Z. Wang, A. Cheng, and G. Li, "Design optimisation of composite bumper beam with variable cross-sections for automotive vehicle," International Journal of Crashworthiness, vol. 22, pp. 1–12, Oct. 2016, doi: http://dx.doi.org/10.1080/13588265.2016.1267552